

# Repairing and Inpainting Damaged Images using Adaptive Diffusion Technique

P.Asواني Kumar<sup>1</sup> | Jorige Venkateswara Rao<sup>2</sup>

<sup>1</sup>Assistant Professor, Department of ECE, Eluru College of Engineering and Technology, Eluru, Andhra Pradesh, India.

<sup>2</sup>PG Scholar, Department of ECE, Eluru College of Engineering and Technology, Eluru, Andhra Pradesh, India.

## To Cite this Article

P.Asواني Kumar and Jorige Venkateswara Rao, "Repairing and Inpainting Damaged Images using Adaptive Diffusion Technique", *International Journal for Modern Trends in Science and Technology*, Vol. 03, Issue 04, 2017, pp. 34-39.

## ABSTRACT

Learning good image priors is of utmost importance for the study of vision, computer vision and image processing applications. Learning priors and optimizing over whole images can lead to tremendous computational challenges. In contrast, when we work with small image patches, it is possible to learn priors and perform patch restoration very efficiently. This raises three questions - do priors that give high likelihood to the data also lead to good performance in restoration? Can we use such patch based priors to restore a full image? Can we learn better patch priors? In this work we answer these questions. We compare the likelihood of several patch models and show that priors that give high likelihood to data perform better in patch restoration. Motivated by this result, we propose a generic framework which allows for whole image restoration using any patch based prior for which a MAP (or approximate MAP) estimate can be calculated. We show how to derive an appropriate cost function, how to optimize it and how to use it to restore whole images. Finally, we present a generic, surprisingly simple Gaussian Mixture prior, learned from a set of natural images. When used with the proposed framework, this Gaussian Mixture Model outperforms all other generic prior methods for image denoising, deblurring and inpainting.

**KEYWORDS:** Gaussian Mixture Model, Image denoising, Deblurring, Damaged Images and Inpainting

Copyright © 2017 International Journal for Modern Trends in Science and Technology  
All rights reserved.

## I. INTRODUCTION

Image priors have become a popular tool for image restoration tasks. Good priors have been applied to different tasks such as image denoising, image inpainting and more, yielding excellent results. However, learning good priors from natural images is a daunting task - the high dimensionality of images makes learning, inference and optimization with such priors prohibitively hard.

### From Patch Likelihoods to Patch Restoration:

For many patch priors a closed form of log likelihood, Bayesian Least Squares (BLS) and Maximum A-Posteriori (MAP) estimates can be easily calculated. Given that, we start with a simple

question: Do priors that give high likelihood for natural image patches also produce good results in a restoration task such as denoising.

In order to provide an answer for this question we compare several popular priors, trained over 50,000  $8 \times 8$  patches randomly sampled from the training set of with their DC removed. We compare the log likelihood each model gives on a set of unseen natural image patches (sampled from the test set of [10]) and the performance of each model in patch denoising using MAP estimates. The models we use here are: Independent pixels with learned marginals (Ind. Pixel), Multivariate Gaussian over pixels with learned covariance (MVG), Independent PCA with learned (non-Gaussian) marginals and ICA with learned

marginals. For a detailed description of these models see the Supplementary Material.

**From Patch Likelihoods to Whole Image Restoration:**

Motivated by the results in Section 2, we now wish to answer the second question of this paper - do patch priors that give high likelihoods perform better in whole image restoration? To answer this question we first need to consider the problem of how to use patch priors for whole image

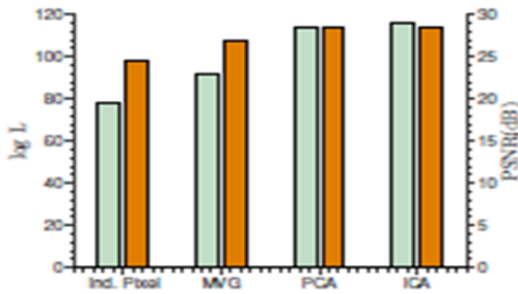


**Fig : Denoising**

**II. PERFORMANCE**

The likelihood of several off-the-shelf patch priors, learned from natural images, along with their patch denoising performance. As can be seen, patch priors that give higher likelihood to the data give better patch denoising performance (PSNR in dB). In this paper we show how to obtain similar performance in whole image restoration.

To illustrate the advantages and difficulties of working with patch priors, consider Figure 2. Suppose we learn a simple patch prior from a given image (Figure 2a). To learn this prior take all overlapping patches from the image, remove their DC component and build a histogram of all patches in the image, counting the times they appear in it. Under this prior, for example, the most likely patch would be flat (because the majority of patches in the original image).

**Framework and Optimization:**

**Expected Patch Log Likelihood – EPLL:**

The basic idea behind our method is to try to maximize the Expected Patch Log Likelihood (EPLL) while still being close to the corrupted image in a way which is dependent on the corruption model. Given an image  $x$  (in vectorized form) we define the EPLL under prior  $p$  as:

$$EPLL_p(x) = \sum_i \log p(P_i x) \tag{1}$$

Where  $P_i$  is a matrix which extracts the  $i$ -th patch from the image (in vectorized form) out of

all overlapping patches, while  $\log p(P_i x)$  is the likelihood of the  $i$ -th patch under the prior  $p$ . Assuming a patch location in the image is chosen uniformly at random, EPLL is the expected log likelihood of a patch in the image (up to a multiplication by  $1/N$ ).

Now, assume we are given a corrupted image  $y$ , and a model of image corruption of the form  $\|Ax - y\|^2$  - We note that the corruption model we present here is quite general, as denoising, image inpainting and deblurring [7], among others, are special cases of it. We will discuss this in more detail in Section 3.1.3. The cost we propose to minimize in order to find the reconstructed image using the patch prior  $p$  is:

$$f_p(x/y) = \frac{\lambda}{2} \|Ax - y\|^2 - EPLL_p(x) \tag{2}$$

Equation 2 has the familiar form of a likelihood term and a prior term, but note that  $EPLL_p(x)$  is not the log probability of a full image. Since it sums over the log probabilities of all overlapping patches, it "double counts" the log probability. Rather, it is the expected log likelihood of a randomly chosen patch in the image.

**Optimization:**

Direct optimization of the cost function in Equation 2 may be very hard, depending on the prior used.

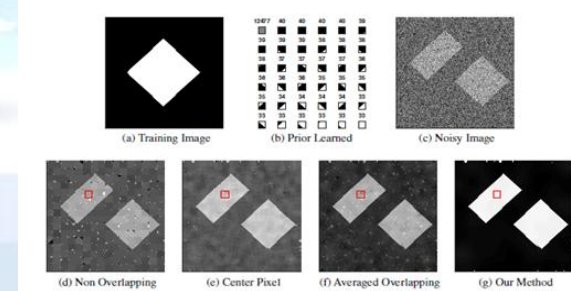


**Fig 2: Optimization using Priors**

alternative optimization method called "Half Quadratic Splitting" which has been proposed recently in several relevant contexts. This method allows for efficient optimization of the cost. In "Half Quadratic Splitting" we introduce a set of patches  $\{z^i\}_1^N$  one for each overlapping patch  $P_i x$  in the image, yielding the following cost function:

$$c_{p,\beta}(x, \{z^i\}/y) = \frac{\lambda}{2} \|Ax - y\|^2 + \sum_i \frac{\beta}{2} (\|P_i x - z^i\|^2) - \log p(z^i) \tag{3}$$

Note that as  $\beta \rightarrow \infty$  we restrict the patches  $P_i x$  to be equal to the auxiliary variables  $\{z^i\}$  and the solutions of Equation 3 and Equation 2 converge. For a fixed value of  $\beta$ , optimizing.

**Related Methods:**

Several existing methods are closely related, but are fundamentally different from the proposed framework. The first related method is the Fields of Experts (FoE) framework by Roth and Black [6]. In FoE, a Markov Random Field (MRF) whose filters are trained by approximately maximizing the likelihood of the training images is learned. Due to the intractability of the partition function, learning with this model is extremely hard and is performed using contrastive divergence. Inference in FoE is actually a special case of our proposed method - while the learning is vastly different, in FoE the inference procedure is equivalent to optimizing Equation 2 with an independent prior (such as ICA), whose filters were learned before hand. A common approximation to learning MRFs is to approximate the log probability of an image as a sum of local marginal or conditional probabilities as in the method of composite likelihood [13] or directed models of images [14]. In contrast, we do not attempt to approximate the global log probability and argue that modeling the local patch marginals is sufficient for image restoration. This points to one of the advantages of our method - learning a patch prior is much easier than learning a MRF. As a result, we can learn a much richer patch prior easily and incorporate it into our framework - as we show later.

Another closely related method is KSVD [3] - in KSVD, one learns a patch based dictionary which attempts to maximize the sparsity of resulting coefficients. This dictionary can be learned either from a set of natural image patches (generic, or global as it is sometimes called) or the noisy image itself (image based). Using this dictionary, all overlapping patches of the image are denoised independently and then averaged to obtain a new reconstructed image. This process is repeated for several iterations using this new estimated image. Learning the dictionary in KSVD is different than learning a patch prior because it may be performed as part of the optimization process (unless the dictionary is learned beforehand from natural images), but the optimization in KSVD can be seen as a special case of our method - when the prior is a sparse prior,

our cost function and KSVD's are the same. We note again, however, that our framework allows for much richer priors which can be learned beforehand over patches - as we will see later on, this boasts some tremendous benefits.

**Patch Likelihoods and the EPLL Framework:**

We have seen that the EPLL cost function (Equation 2) depends on the likelihood of patches. Going back to the priors from Section 2 we now ask - do better priors (in the likelihood sense) also lead to better whole image denoising with the proposed EPLL framework? Figure 4 shows the average PSNR obtained with 5 different images from the Berkeley training set, corrupted with Gaussian noise at  $\sigma = 25$  and denoised using each of the priors in section 2. We compare the result obtained using simple patch averaging (PA) and our proposed EPLL framework.

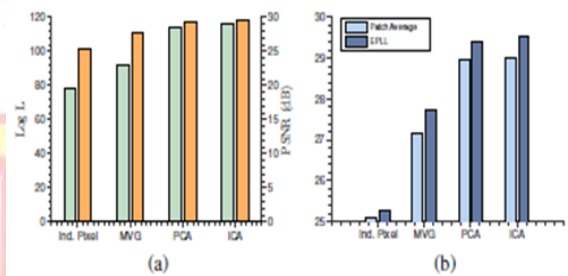


**Fig 4: Image Denoising Performance (a) Whole image denoising with the proposed framework with all the priors discussed in Section (b) Note how the EPLL framework improves performance significantly when compared to simple patch averaging (PA)**

**Gaussian Mixture Prior:**

We learn a finite Gaussian mixture model over the pixels of natural image patches. Many popular image priors can be seen as special cases of a GMM but they typically constrain the means and covariance matrices during learning. In contrast, we do not constrain the model in any way—we learn the means, full covariance matrices and mixing weights, over all pixels. Learning is easily performed using the Expectation Maximization algorithm (EM). With this model, calculating the log likelihood of a given patch is trivial:

$$\log p(x) = \log \left( \sum_{k=1}^K \pi_k N(x/\mu_k, \Sigma_k) \right) \quad (5)$$

Where  $\pi_k$  are the mixing weights for each of the mixture component and  $\mu_k$  and  $\Sigma_k$  are the corresponding mean and covariance matrix.

Given a noisy patch  $y$ , the BLS estimate can be calculated in closed form (as the posterior is just another Gaussian mixture) [1]. The MAP estimate, however, can not be calculated in closed form. To tackle this we use the following approximate MAP estimation procedure:

1. Given noisy patch  $y$  we calculate the conditional mixing weights  $\pi'_k = P(k/y)$ .
2. We choose the component which has the highest conditional mixing weight  $k_{\max} = \max_k \pi'_k$ .
3. The MAP estimate  $\hat{x}$  is then a Wiener filter solution for the  $k_{\max}$ -th component:

$$\hat{x} = (\Sigma_{k_{\max}} + \sigma^2 I)^{-1} (\Sigma_{k_{\max}} y + \sigma^2 I \mu_{k_{\max}})$$

Model	Log L	Patch Restoration		Image Restoration	
		BLS	MAP	PA	EPLL
Ind. Pixel	78.26	25.54	24.43	25.11	25.26
MVG	91.89	26.81	26.81	27.14	27.71
PCA	114.24	28.01	28.38	28.95	29.42
ICA	115.86	28.11	28.49	29.02	29.53
GMM	164.52	30.26	30.29	29.59	29.85

**Table 1: Difference Between Patch And Image Restoration**

GMM model performance in log likelihood (Log L), patch denoising (BLS and MAP) and image denoising (Patch Average (PA) and EPLL, the proposed framework) - note that the performance is better than all priors in all measures. The patches, noisy patches, images and noisy images are the same as in Figure 1 and Figure 4. All values are in PSNR (dB) apart from the log likelihood.

### Comparison:

We learn the proposed GMM model from a set of  $2 \times 10^6$  patches, sampled from [10] with their DC removed. The model is with learned 200 mixture components with zero means and full covariance matrices. We also trained GMMs with unconstrained means and found that all the means were very close to zero. As mentioned above, learning was performed using EM. Training with the above training set takes around 30h with unoptimized MATLAB code<sup>1</sup>. Denoising a patch with this model is performed using the approximate MAP procedure described. Having learned this GMM prior, we can now compare its performance both in likelihood and denoising with

the priors we have discussed thus far in Section 1 on the same dataset of unseen patches. Table 1 shows the results obtained with the GMM prior - as can be seen, this prior is superior in likelihood, patch denoising and whole image denoising to all other priors we discussed thus far.

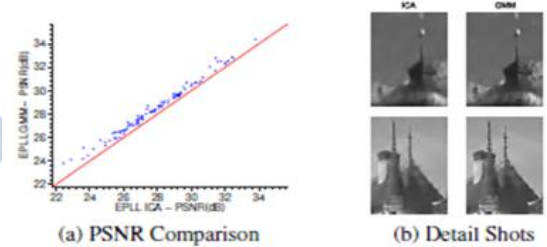


**Fig : PSNR Comparison**

Comparison of the performance of the ICA prior to the high likelihood GMM prior using EPLL and noise level  $\sigma = 25$ . 5a depicts a scatter plot of PSNR values obtained when denoising 68 images from [10]. Note the superior performance of the GMM prior when compared to ICA on all images. 5b depicts a detail shot from two of the images - note the high visual quality of the GMM prior result. The details are best seen when zoomed in on a computer screen.

### Comparison to State-Of-The-Art Methods:

We compare the performance of EPLL with the proposed GMM prior with leading image restoration methods - both generic and image based. All the experiments were conducted on 68 images from the test set of the Berkeley Segmentation Database [10]. All experiments were conducted using the same noisy realization of the images. In all experiments we set  $\lambda = N/\sigma^2$ , where  $N$  is the number of pixels in each patch. We used a patch size of  $8 \times 8$  in all experiments. For the GMM prior, we optimized (by hand) the values for  $\beta$  on the 5 images from the Berkeley training set - these were set to  $\beta = 1/\sigma^2$  [1, 4, 8, 16, 32, 64]. Running times on a Quad Core Q6600 processor are around 300s per image with unoptimized MATLAB code.

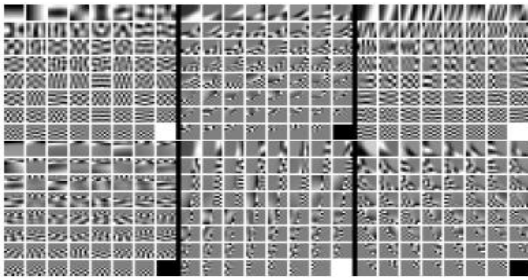
$\sigma$	KSVGD	FoE	GMM-EPLL	$\sigma$	KSVD	BM3D	LLSC	GMM-EPLL
15	30.67	30.18	31.21	15	30.59	30.87	31.27	31.21
25	28.28	27.77	28.71	25	28.20	28.57	28.70	28.71
50	25.18	23.29	25.72	50	25.15	25.63	25.73	25.72
100	22.39	16.68	23.19	100	22.40	23.25	23.15	23.19

(a) Generic Priors

(b) Image Based Methods

**Table 2: Comparison of Generic and Image based methods Prior**

Summary of denoising experiments results. Our method is clearly state-of-the-art when compared to generic priors, and is competitive with image based method such as BM3D and LLSC which are state-of-the-art in image denoising.



Eigenvectors of 6 randomly selected covariance matrices from the learned GMM model, sorted by eigenvalue from largest to smallest. Note the richness of the structures - some of the eigenvectors look like PCA components, while others model texture boundaries, edges and other structures at different orientations.

**Generic Priors:**

We compare the performance of EPLL and the GMM prior in image denoising with leading generic methods - Fields of Experts [6] and KSVD [3] trained on natural image patches (KSVDG). The summary of results may be seen in Table 2a - it is clear that our method outperforms the current state-of-the-art generic methods.

**Image Based Priors:**

We now compare the performance of our method (EPLL+GMM) to image specific methods - which learn from the noisy image itself. We compare to KSVD, BM3D [5] and LLSC [8] which are currently the state-of-the-art in image denoising. The summary of results may be seen in Table 2b. As can be seen, our method is highly competitive with these state-of-the-art method, even though it is generic. Some examples of the results may be seen in Figure 6.

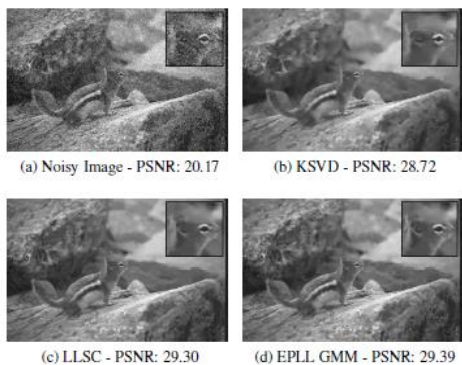


**Fig 6 : Denoised Images**

**Image Deblurring:**

While image specific priors give excellent performance in denoising, since the degradation of different patches in the same image can be "averaged out", this is certainly not the case for all image restoration tasks, and for such tasks a generic prior is needed. An example of such a task is image deblurring. We convolved 68 images from the Berkeley database (same as above) with the blur kernels supplied with the code of [7]. We then added 1% white Gaussian noise to the images, and attempted reconstruction using the code by [7] and our EPLL framework with GMM prior. Results are superior both in PSNR and quality of the output, as can be seen in Figure 8.



	Krishnan et al.	EPLL-GMM
Kernel 1 17 × 17	25.84	27.17
Kernel 2 19 × 19	26.38	27.70

**Fig 8: Deblurring experiments**

**III. RESULTS AND CONCLUSION**

By applying above discussed methods the results are of the corrupted images are as follows:

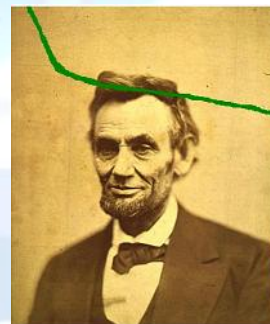


**Fig 8.1(a) corrupted image**

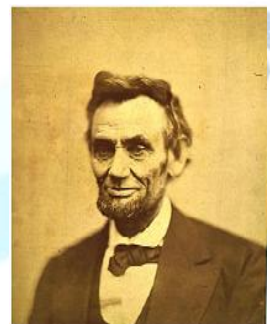


**Fig 8.1(b) restored image**



**Fig 8.2 (a) corrupted image**



**Fig 8.2 (b) restored image**

#### **IV. CONCLUSION**

We have presented a new system for meaningful structure extraction from texture. Our main contribution is twofold. First, we proposed novel variation measures to capture the nature of structure and texture. We have extensively evaluated these measures and conclude that they are indeed powerful to make these two types of visual information separable in many cases. Second, we fashioned a new optimization scheme to transform the original non-linear problem to a set of sub problems that are much easier to solve quickly. Several applications making use of these images and drawings were proposed. Our method does not need prior texture information. It could, thus, mistake part of structures as texture, if they are visually similar in scales. One example is shown in Figure 15, where structures are not all preserved. It is because the scale and shape of these edges are overly close to those of the underlying texture; significantly obscure the difference from the statistical perspective.

#### **REFERENCES**

- [1] M. Bertalmío, G. Sapiro, V. Caselles, and C. Ballester, "Image inpainting," in SIGGRAPH, 2000, pp. 417-424. (Pubitemid 32394006)
- [2] T. F. Chan and J. Shen, "Local inpainting models and tv inpainting," SIAM Journal on Applied Mathematics, vol. 62, no. 3, pp. 1019-1043, 2001.
- [3] T. F. Chan and J. Shen, "Non-texture inpainting by curvature-driven diffusions (cdd)," J. Visual Comm. Image Rep, vol. 12, pp. 436-449, 2001. (Pubitemid 34091699)
- [4] A. Efros and T. Leung, "Texture synthesis by nonparametric sampling," in International Conference on Computer Vision, 1999, pp. 1033-1038.
- [5] M. Bertalmío, L. A. Vese, G. Sapiro, and S. Osher, "Simultaneous structure and texture image inpainting," IEEE Transactions on Image Processing, vol. 12, no. 8, pp. 882-889, 2003.
- [6] A. Criminisi, P. Pérez, and K. Toyama, "Region filling and object removal by exemplar-based image inpainting," IEEE Transactions on Image Processing, vol. 13, no. 9, pp. 1200-1212, 2004.
- [7] Y. Wexler, E. Shechtman, and M. Irani, "Space-time completion of video," IEEE Transactions on Pattern Analysis and Machine Intelligence, vol. 29, pp. 463-476, 2007.
- [8] M. Zmiri-Yaniv, M. Ofry, A. Bruker, and T. Hassner, "Image completion,"